Electronic Supplementary Material (ESI) for Chemical Science.

Micrometer-Scale Transient Ion Transport at Functionalized Micropipette for Real-Time pH Assay in Rat Brain

Kailin Zhang,[a,c] Huan Wei,[a,c] Tianyi Xiong,[a,c] Yanan Jiang,[a] Wenjie Ma,[a] Fei Wu,[a] Ping Yu,[*a,c] and Lanqun Mao[a,b,c]

[a]*Beijing National Laboratory for Molecular Sciences (BNLMS), Key Laboratory of Analytical Chemistry for Living Biosystems, Institute of Chemistry, the Chinese Academy of Sciences (CAS), CAS Research/Education Center for Excellence in Molecular Science, Beijing 100190, China. E-mail: yuping@iccas.ac.cn.*

[b]*College of Chemistry, Beijing Normal University, Beijing 100875, China.*

[c]*College of Chemical Sciences, University of Chinese Academy of Sciences, Beijing 100049, China.*

Supplementary Figures

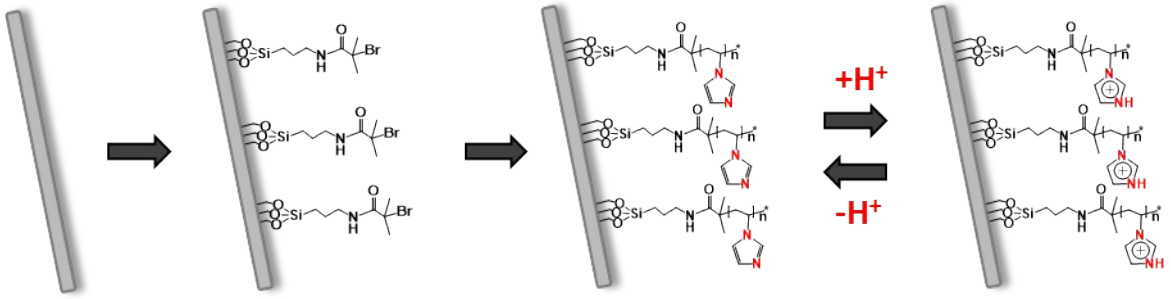

Figure S1. PvimB-modified micropipettes by surface-initiated atom transfer radical polymerization.

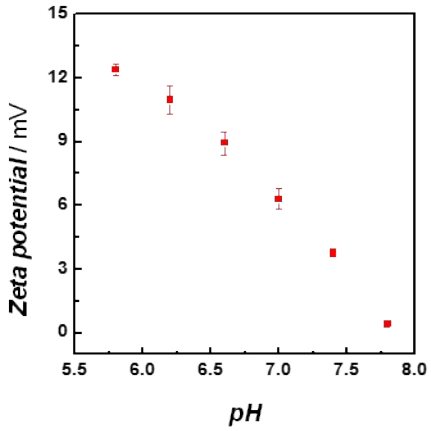

Figure S2. Zeta potential of PvimB-modified SiNPs at different pH in 100 mM NaCl containing 50 mM phosphate.

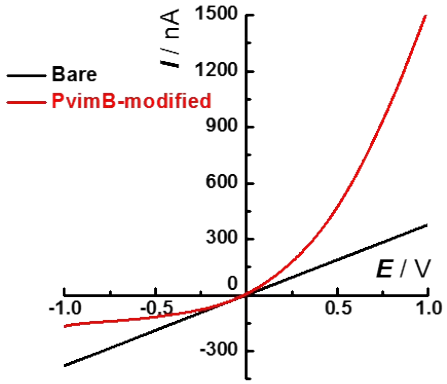

Figure S3. *I-V* curves obtained at bare (black curve) and PvimB-modified (red curve) micropipette in 100 mM NaCl containing 50 mM phosphate (pH 5.8). Scan rate was 50 mV s^{-1}.

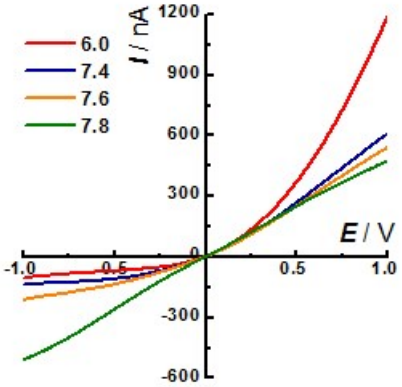

Figure S4. *I-V* curves obtained at PvimB-modified micropipette with different pH in 100 mM NaCl containing 50 mM phosphate. Scan rate was 50 mV s^{-1}.

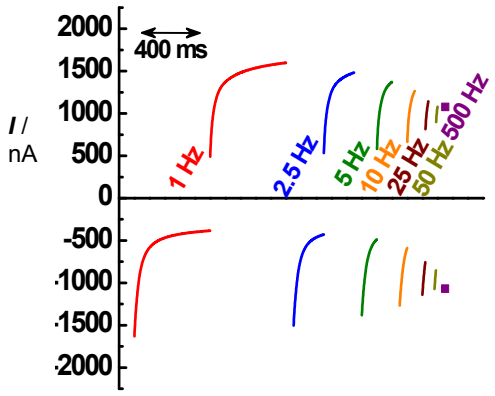

Figure S5. Current trace obtained at a PvimB-modified micropipette under the polarization of pulse potential with different frequency ($+V_{step}$ = +1 V, $-V_{step}$ = -1 V).

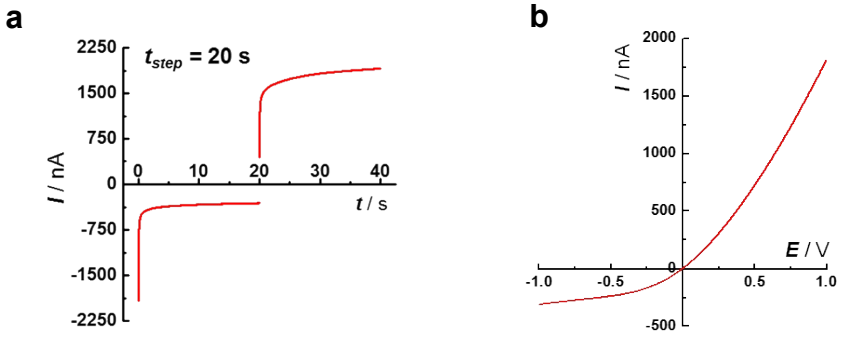

Figure S6. (a) Ion current traces obtained at a PvimB-modified micropipette in pH 5.8 solution under the polarization of pulse potential (t_{step} = 20 s). The values of $+V_{step}$ and $-V_{step}$ were +1 V and -1 V, respectively. (b) *I-V* curve obtained at a PvimB-modified micropipette in 100 mM NaCl containing 50 mM phosphate (pH 5.8). Scan rate was 50 mV s^{-1}.

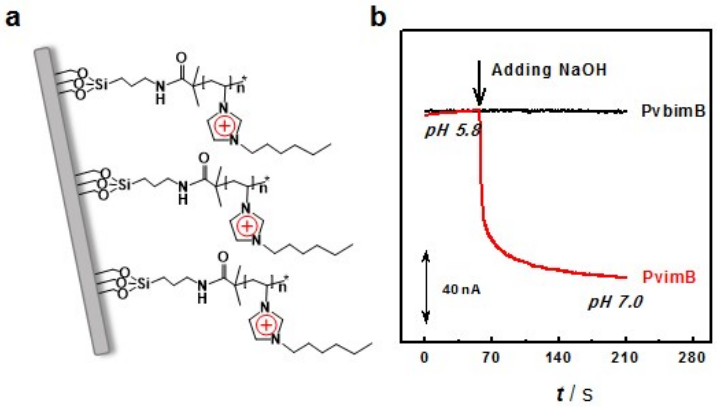

Figure S7. (a) The poly(1-vinyl-3-butylimidazolium) brushes (PvbimB)-modified micropipette. (b) The end current response obtained at PvbimB-modified (black curve) and PvimB-modified (red curve) micropipette towards pH varying from 5.8 to 7.0. The electrolyte solution was 100 mM NaCl containing 50 mM phosphate.

Finite element simulation was carried out with COMSOL Multiphysics 5.4a (COMSOL Inc.) with a high-performance server. And a steady state model for polyelectrolyte brush modified micropipettes was carried out according to previous reports: We consider a 50-μm-long conical (half cone angle θ=3°) micropore with 10 μm orifice (r= 5 μm) immersed in a reservoir. And a uniform PimB layer was end-grafted around the inner wall of the micropipette. Assuming that the PimB layer is ion-penetrable and homogeneously structured with a uniform thickness of L_c=300 nm. And an external bias V was applied to the pipettes with 2 electrodes in the reservoirs. Owing to the axial symmetric characteristics of the micropipettes, 2D axial symmetric model (r, z) was adopted in this work. And a continuum Poisson-Nernst-Planck was employed to describe the ion transport behaviors in the pipettes:

$$-\nabla^2\boldsymbol{\phi} = -\frac{f\rho_c + \rho_e}{\varepsilon},\ f=1 \text{ or } 0.$$

$$\boldsymbol{J}_i = -D_i\nabla c_i + \frac{z_i F}{RT}\nabla^2\boldsymbol{\phi},$$

Where $\boldsymbol{\phi}$, ρ_c, ρ_e and ε are the local electrical potential, charge density in the PimB layer, charge density of the mobile ions ($\rho_{e=}\sum_i z_i c_i$) and the dielectric constant of the system respectively; And $\boldsymbol{J_i}$, D_i, C_i, z_i, are the total ion flux, diffusion coefficient, local concentration and charge of species *i* respectively; R, T and and F are the gas constant, tempreature and faraday constant respectively. Based on the detailed boundary condtions illustrated in Figure S8, electric field distribution in the modified pipettes could be numerically figured out in Figure S9.

The FEM simulation consisted 3723920 freedoms, and finer meshes were generated in the polyelectrolyte layer to accurately describe the electrical double layer and the transport behaviors at the orifice. Mesh-refinement test was performed strictly to ensure all results are fully converged and mesh-independent.

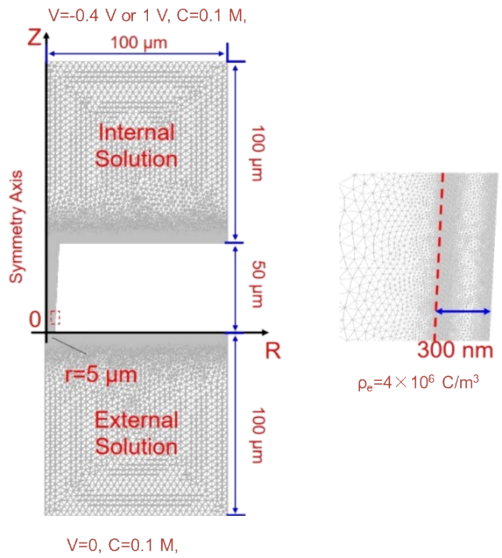

Figure S8. Geometric structure, detailed boundary conditions and mesh distribution of the FEM simulation to the modified micropipettes.

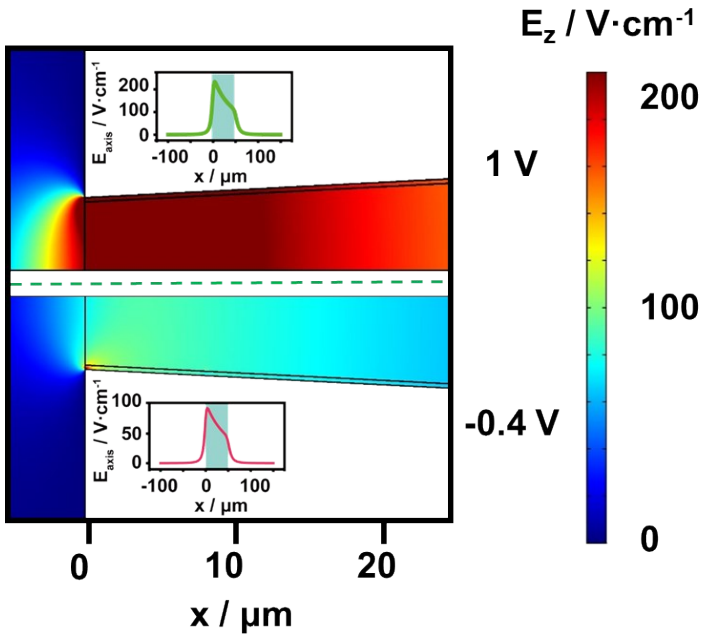

Figure S9. Simulated axial electrical field intensity of a 5-μm-radius polyelectrolyte modified micropipette under 1 V and -0.4 V bias potential. The inner plots shown the electrical field distribution at x axis.

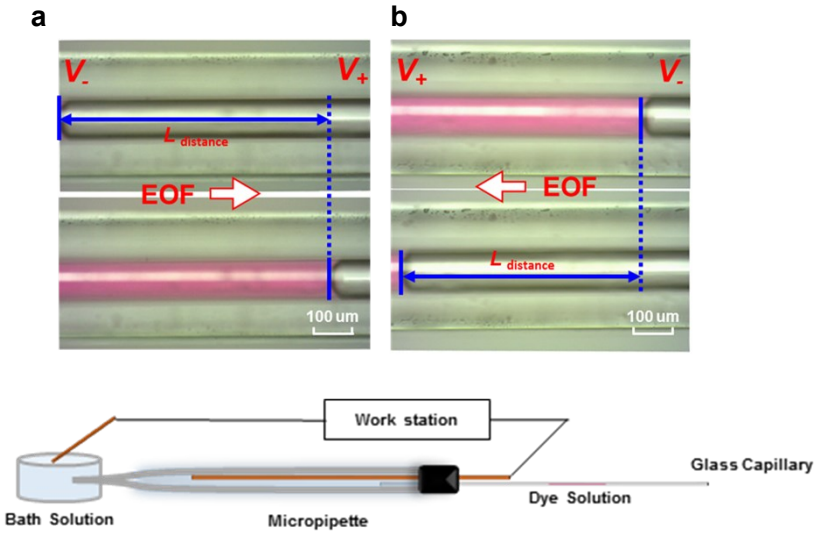

Figure S10. Schematic illustration of the experimental equipment for measurement of EOF velocity. A small volume rhodamine solution was sealed in the the glass capillary, which was used for indicating the velocity of fludic flow. The electrolyte solution was 100 mM NaCl containing 50 mM phosphate (pH 5.8). The velocities of EOF under different applied potentials were calculated and shown in Table S1.

Table S1. The velocity of EOF (v_{EOF}) under different bias potentials at pH 5.8.

	+1 V	0.4 V	-1 V	-0.4 V
v_{EOF} (μm/s)	15 ± 1.5	5.4 ± 0.92	26 ± 2.0	8.2 ± 1.8

In this table, all the values were obtained according to the following equation：

$$v_{EOF} = \frac{\Delta x}{t} \cdot \frac{r_c^2}{r_p^2}$$

Where r_c and r_p are the radius of the capillary and the pipette, respectively, Δx is the movement of the rhodamine solution and Δt is the time duration. Herein, r_p=5 μm, r_c=50 μm, t = 3600 s, and Δx at different potential was measured by the setup in Figure S8.

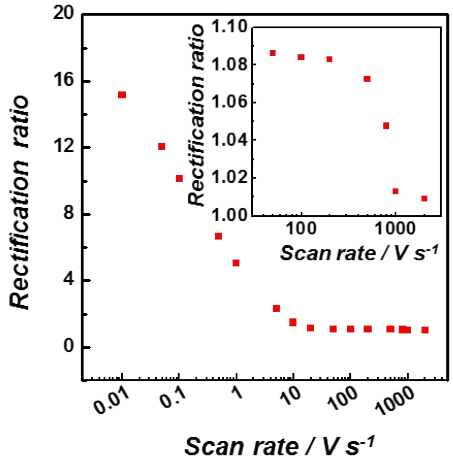

Figure S11. Rectification ratios plotted as functions of the scan rate at the PvbimB-modified micropipette. Inset: rectification ratio plotted as functions of the scan rate from 50 to 2000 V/s. The electrolyte solution was 100 mM NaCl containing 50 mM phosphate (pH 5.8).

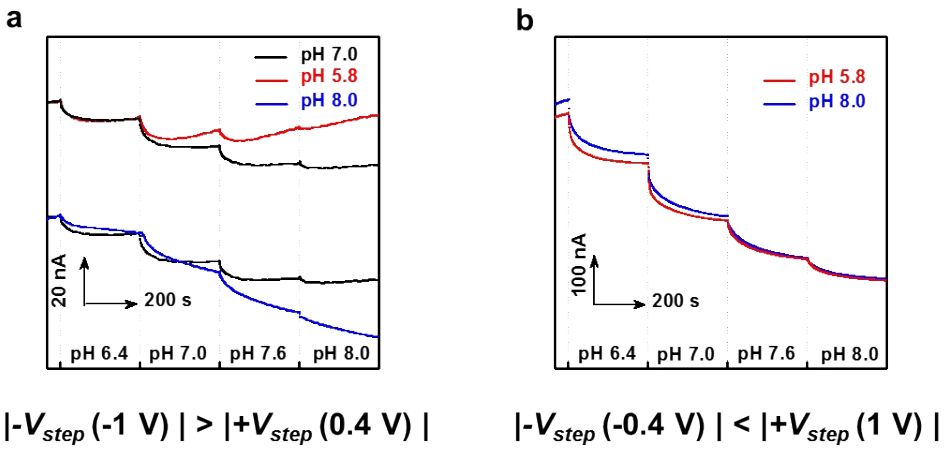

Figure S12. Positive end current obtained at PvimB-modified micropipette towards varying pH from 6.4 to 8.0 under the polarization of different pulse potential: (a) $+V_{step}$, $-V_{step}$ and t_{step} were +0.4 V, -1 V and 0.2 s, respectively; (b) $+V_{step}$, $-V_{step}$ and t_{step} were +1 V, -0.4 V and 0.2 s, respectively. The pH of the pipette solution is 5.8 (red line), 7.0 (black line) and 8.0 (blue line). The electrolyte solution was 100 mM NaCl containing 50 mM phosphate.

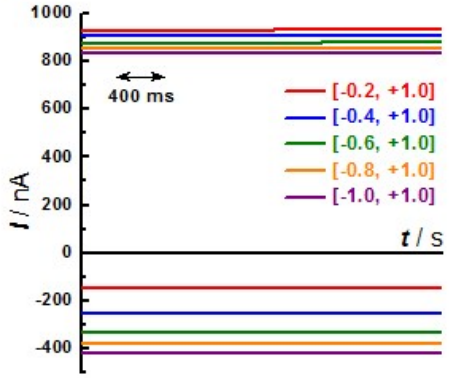

Figure S13. Positive and negative current trances with the different applied -V_{step} ($|-V_{step}| < |+V_{step}| = 1$V) at the PvimB-modified micropipette. The electrolyte solution was 100 mM NaCl containing 50 mM phosphate and the pipette solution was 100 mM NaCl containing 50 mM phosphate (pH 7.0)

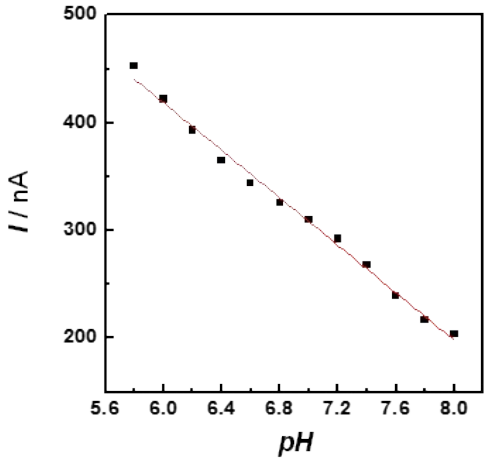

Figure S14. Post-calibration curve of PvimB-modified micropipette after in vivo experiments. The values of +V_{step}, -V_{step} and t_{step} were +1 V, -0.4 V and 0.2 s, respectively. The pipette solution is aCSF (pH = 7.4). The electrolyte solution was 100 mM NaCl containing 50 mM phosphate.

Table S2. Performance of the reported pH *in vivo* microsensor.

	Response time	Diameter (μm)	Selectivity	Stability	Sensitivity
ISE[1]	< 1 s	1~25	High	N/A	~59 mV/pH
FSCV[2]	~100 ms	7	N/A	~ 90 s	~-110 nA/pH
IrO_x[3]	~5 s	80~500	No interference when added some bivalent cations	0.6 mV/h	62~85 mV/pH
CV/DPV[4]	N/A	>10	High	5 mV (500 cycles)	~59 mV/pH
This work	1~ 800 ms	1~10	High	~3.3 nA/h	~200 nA/pH

[1] a) W. A. C. Mutch, A. J. Hansen, *J. Cereb. Blood Flow Metab.* **1984**, *4*, 17-27; b) F. Zhao, Y. Liu, H. Dong, S. Feng, G. Shi, L. Lin, Y. Tian, *Angew. Chem. Int. Ed.* **2020**, *59*, 10426-10430; c) J. Hao, T. Xiao, F. Wu, P. Yu, L. Mao, *Anal. Chem.* **2016**, *88*, 11238-11243.

[2] a) B. J. Venton, D. J. Michael, R. M. Wightman, *J. Neurochem.* **2003**, *84*, 373-381; b) P. Takmakov, M. K. Zachek, R. B. Keithley, E. S. Bucher, G. S. McCarty, R. M. Wightman, *Anal. Chem.* **2010**, *82*, 9892-9900.

[3] a) G. Papeschi, S. Bordi, M. Carla, L. Criscione, F. Ledda, *J. Med. Eng. Technol.* **1981**, *5*, 86-88; b) M. D. Johnson, O. E. Kao, D. R. Kipke, *J. Neurosci. Methods* **2007**, *160*, 276-287.

[4] a) J. Zhou, L. Zhang, Y. Tian, *Anal. Chem.* **2016**, *88*, 2113-2118; b) L. Liu, F. Zhao, W. Liu, T. Zhu, J. Z. H. Zhang, C. Chen, Z. Dai, H. Peng, J.-L. Huang, Q. Hu, W. Bu, Y. Tian, *Angew. Chem. Int. Ed.* **2017**, *56*, 10471-10475; c) W. Liu, H. Dong, L. Zhang, Y. Tian, *Angew. Chem. Int. Ed.* **2017**, *56*, 16328-16332.